SCIENCE CHINA
Earth Sciences

Progress of Projects Supported by NSFC
• RESEARCH PAPER •

June 2013 Vol.56 No.6: 901–912
doi: 10.1007/s11430-013-4595-4

Neoproterozoic sedimentary facies and glacial periods in the southwest of Tarim Block

TONG QinLong[1,2], WEI Wei[1] & XU Bei[1*]

[1] *Key Laboratory of Orogenic Belts and Crustal Evolution, Ministry of Education, School of Earth and Space Sciences, Peking University, Beijing 100871, China;*
[2] *National Key Laboratory of Remote Sensing Information and Image Analysis Technology, Beijing Research Institute of Uranium Geology, Beijing 100029, China*

Received March 19, 2012; accepted August 22, 2012; published online April 15, 2013

Based on the analysis of sedimentary facies and chemical index of alteration (CIA) in Nanhua and Ediacaran Systems in the southwest of Tarim Block, some features of glacial records in Neoproterozoic become more clear. Six sedimentary facies have been divided in the study area, including alluvial fan facies, lacustrine facies, glacial facies, littoral facies, neritic facies, and lagoonal facies, showing that this area underwent a process from continent to marine, with mainly littoral and neritic sedimentation. Two cold events have been recognized by analysis of CIA values in the study area, called Bolong and Yutang glaciation, respectively. They present as thick-layer tillite deposition in the Bolong Formation and thin-layer tillite deposition in the Yutang Formation, respectively. The Bolong glacial period in the study area can be correlated to the Yulmeinak glacial period in Aksu area, Tereeken glacial period in Qurugtagh area, and the Nantuo glacial period in South China, which is equivalent to the universally acknowledged Marinoan glacial period. The Yutang glacial period can be correlated to the Hankalchough glacial period in Qurugtagh, which is equivalent to Gaskers glaciation in Newfoundland.

Tarim Block, Neoproterozoic, sedimentary facies, chemical alteration index, tillite

Citation: Tong Q L, Wei W, Xu B. Neoproterozoic sedimentary facies and glacial periods in the southwest of Tarim Block. Science China: Earth Sciences, 2013, 56: 901–912, doi: 10.1007/s11430-013-4595-4

Neoproterozoic glacial events have raised many questions that need to be answered. For example, how many times did the glacial events occur? When did each glacial event begin and end? What is the relationship between a glacial event and climate change? What is the relationship between a glacial event and the break-up of supercontinent, the evolution of life and so on [1–6]? With the hypothesis of "Snowball Earth" by Hoffman et al. [7], more and more geologists are increasingly interested in researches about Neoproterozoic "Snowball" events and the global climate changes at that time. At present, four or five glacial periods are universally acknowledged [7, 8]. Two worldwide glacial periods are suggested. One is called Sturtian, which occurred at about 717–685 Ma [9, 10], and the other, Marinoan, at about 657–635 Ma [11, 12]. Besides, an older glaciation in Namibia and Zambia, called Kaigas glaciation, occurred at 765–735 Ma [13, 14], and a younger glaciation in Newfoundland, called Gaskiers glaciation, occurred at 580–575 Ma [15]. Two Neoproterozoic glaciations have been confirmed in South China, including Chang'an glaciation, which is equivalent to the Sturtian glaciation, and Nantuo glaciation, which is equivalent to the Marinoan glaciation [11, 16, 17]. In Quruktag area, the northeast of Tarim Block, four Neoproterozoic glacial events have been recognized, including Bayixi, Altungal, Tereeken, and Hangelchaok glaciations [18–20]. In Aksu area, the northwest of Tarim Block, two glacial periods are called Qiaoenbunak and Yuermeinak glaciation respectively [21–24].

The main method of distinguishing different glacial pe-

*Corresponding author (email: bxu@pku.edu.cn)

riod is volcanic zircon dating, and their ages can be used to constrain the time of the start and end of glaciations. Besides, some researchers found that chemical index of alteration (CIA) can also distinguish different glacial period, because the values of CIA in glacial and interglacial epoch are different. Generally, the former are lower than the latter. Accordingly, we can divide the numbers of glacial cycle in different area and infer the climate change at that time. For example, Dobrzinski et al. [25] used major and trace rare element geochemistry to evaluate the environment conditions prevailing during the glaciations in South China. Through analyzing the values of CIA of fine clastic rocks, they suggested there must exist an interglacial period in the big glaciation in Nanhua System. Rieu et al. [26] also used the values of CIA and MIA to divide three glacial periods in Neoproterozoic in Hadash area. They claimed that the cold climate modes of the Cryogenian were cyclical, instead of the whole earth being covered by ice [7]. Goldberg et al. [27] carefully discussed the application of CIA in paleoclimate, and analyzed the major elements of claystone and shale in the Parana Basin in Brazil, and the results were in accord with the evidence from sedimentology and paleontology. Therefore, they considered that the values of CIA can reflect the climate change very well if reasonably used. Likewise, Feng et al. [28, 29] and Wang et al. [30] distinguished two processes of climate change that were from cold to warm and humid in South China through the CIA analysis. Liu et al. [31] distinguished four glacial periods in Quruktag area through CIA analysis. Ding et al. [32] utilized the values of CIA to prove that those tillites deposited in different horizons in Ediacaran Talisayi Formation, actually, were the sedimentation in the same glaciation.

There are excellent Neoproterzoic glacial depositions in the southwest of Tarim Block. But the researches about them are relatively few. Previous studies were concentrated on magmatism, which was related to the breakup of Rodinia supercontinent and the essential features of tillite [33–37]. On the basis of analysis of sedimentary features and facies, by means of the analysis of the chemical index of alteration, we intend to clarify the change of sedimentary environment and the periods of glaciation in Neoproterozoic in the study area, and then make comparisons with those coeval glaciations in Aksu, Quruktag and South China.

1 Geological setting and strata system

The study area is located near the 100 km road sign of Sinkiang-Tibet road, belonging to the Tiekelik area of South Tarim stratum subarea of Tarim stratum area (Figure 1(a)). The Precambrian stratigraphic sequences had been set up by No. 13 geological team in the late 1950s. Geologists of Xinjiang No. 2 Geological Team and Xinjiang Geological Minerals Bureau particularly measured the Neoproterozoic stratigraphic sections in the northern slope of the western Kunlun Mountains in the 1980s–1990s. The strata in Nanhua-

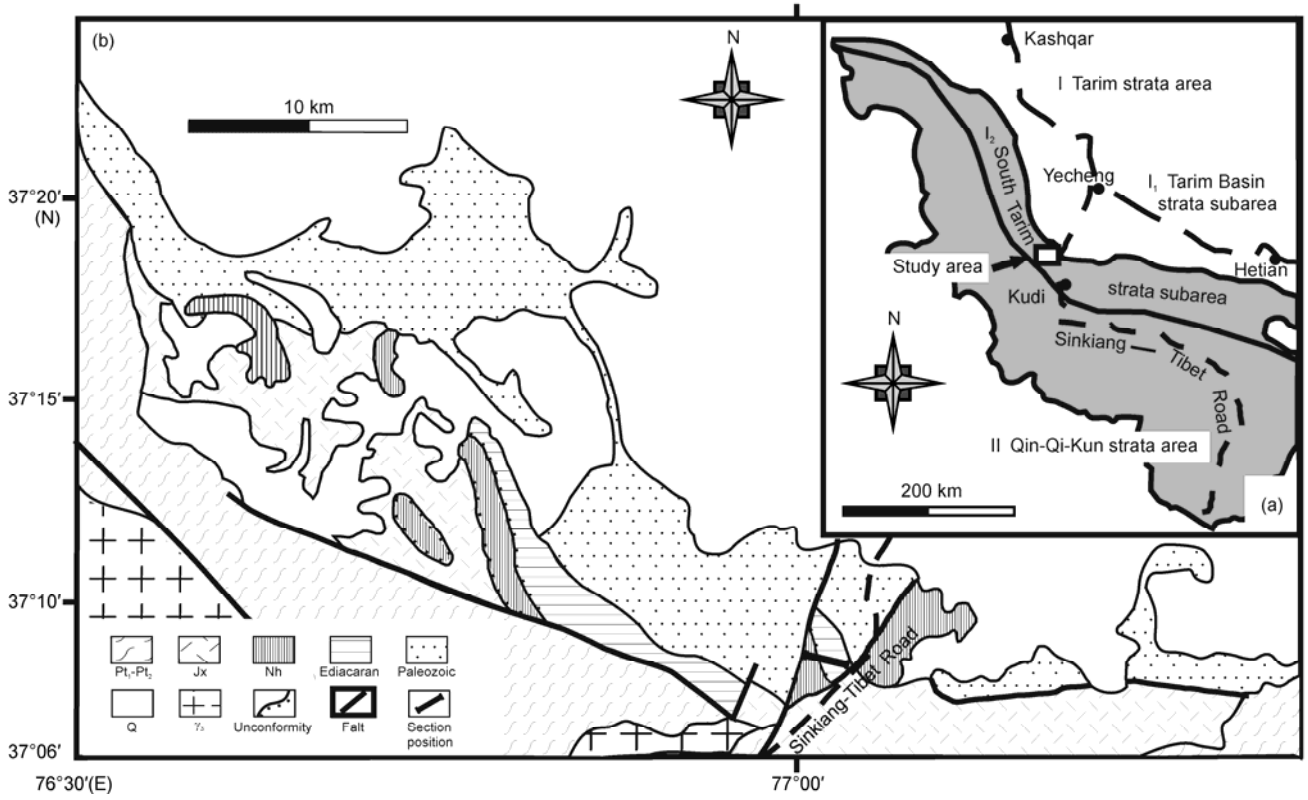

Figure 1 (a) Precambrian stratum subareas in the western Kunlun Mountains; (b) sketch geological map in Yecheng area, Xinjiang.

Table 1 Neoproterozoic strata in Yecheng area (* glacial strata)

Era	Period	Horizon	
Paleozoic	Devonian	Qizilafu Gr.	
Neoproterozoic	Ediacaran	Kezisuhum Fm.	
		Kuerkake Fm.	
	Nanhua	Qiakemakelike Gr.	Yutang Fm.*
			Kelixi Fm.
			Bolong Fm.*
			Yalaguz Fm.
	Qingbaikouan	Sukuluoke Fm.	

Ediacaran had been divided into six formations; from bottom to top, they were Yalaguz, Bolong, Kelixi, Yutang, Kuerkake, and Kezisuhum formations. Glacial diamictite can be observed in the Bolong and Yutang formations [33, 34] (Table 1).

The lower part of 370 m thick Yalaguz Formation mostly comprises purple and thick layer polymictic conglomerate with lamina mudstone and sandstone, and unconformably overlies the Sukuluoke Group in Qingbaikou System. The upper part of this formation consists of many cycles of greyish-green siltstone and purple lamina siltstone. The Bolong Formation mostly comprises thick layer (about 185 m) glacial diamictites. Dropstone structures occurred in the fine clastic rocks at the end of glacial diamictites. The 339 m thick Kelixi Formation, as a whole, consists of two coarsening upward cycles, which contain siltstone, mudstone and fine clastic rocks in the lower part and purple gritstone to conglomerate in the upper part of every cycle. The Yutang Formation consists of glacial diamictite at the bottom, thick layer gritstone in the middle part, and cycles of siltstone and mudstone in the upper part, with a total thickness of about 35 m. It unconformably underlies pebbly gritstone of the Ediacaran Kuerkake Formation. The Kuerkake Formation mainly comprises coarse clastic rocks and intercalations of lamina siltstone and silty shale, which reaches more than 200 m thick. The Kezisuhum Formation (thickness > 90 m) consists of cycles of sandstone and mudstone at the bottom, gypsum-bearing gritstone in the middle part, and thick layer mudstone in the top, and it unconformably underlies the Devonian Qizilafu Group.

2 Sampling and sample analysis

We measured the Neoproterozoic stratigraphic sections in the study area and analyzed the sedimentary environment and facies. Meanwhile, 27 samples were collected for the analysis of CIA. Among them, 9 samples were collected from the Yalaguz Formation, including 7 shales and 2 siltstones. Six samples were collected from the Kelixi Formation (4 mudstones and 2 shales). Five samples were collected from the Yutang Formation (4 mudstones and 1 shales). Two siltstones were collected from the Kuerkake Formation and five mudstones were collected from the Kezisuhum Formation.

Major elements were tested in the Key Laboratory of Orogenic Belts and Crustal Evolution, Ministry of Education, School of Earth and Space Sciences, Peking University. All of those samples are crushed coarsely, cleaned by deionized water and polished to 200-mesh, and then are put into drying oven to dry. After that, 1 g sample was weighed in the crucible and heated for one hour at 680°C in a muffle furnace to get the loss on ignition (LOI). 4 g mixed solvent of lithium tetraborate, lithium metaborate and lithium fluoride and 0.4 g sample, were mixed in a platinum crucible with 4–5 drops Saturated brominated amine, then melted on the HMS-I-XZ and changed into homogeneous sheet glass. Major elements of the sheet glass were analyzed on the sequential X-ray fluorescence spectrometer. GSR5 and GSR2 were used as guide samples. The testing results are showed in Table 2.

3 Sedimentary facies analysis

Six types of sedimentary facies have been recognized in the study area by comprehensive analysis of strata features, such as lithology, sedimentary structures and so on. They are alluvial fan, lacustrine, glacial, littoral, neritic, and lagoonal facies.

3.1 Alluvial fan facies

The lower part of the Yalaguz Formation develops alluvial fan facies, which mainly comprises purple and thick-layer polymictic conglomerate and intercalations of purple and thin-layer mudstone or siltstone. The total thickness of this part is about 370 m. It was interpreted as molasse formation [34]. Gravels in the conglomerate include silicolite, limestone, granite, quartz clast and so on. Grain size of gravels varies in mm- to cm-sized. Hyporound-round shape of the gravels indicates that they underwent a long-distance transportation. The bedding is not clear, presenting massive structure as a whole. Locally, sandstone lens can be observed on the top of this part.

3.2 Lacustrine facies

The middle and upper parts of the Yalaguz Formation, which consists of laminated siltstone, silty shale and other clasts, develop lacustrine facies. One distinct feature is that the amaranthine and greyish-green laminated siltstone deposited alternately. The amaranthine siltstone or silty shale is characterized by high grade of maturity, good sorting, and abrasion. Main clastic composition is quartz and feldspar. Horizontal bedding can be observed in the mud interval, probably representing lakeshore facies. With straight and mm-sized lamina and horizontal bedding, the greyish-green laminated siltstone shows high textural maturity and repre-

Table 2 Data of major elements and values of CIA and ICV of fine clastic rocks of Nanhua-Ediacaran in Yecheng

Horizon		Sample No.	Lithology	SiO_2 (%)	Al_2O_3 (%)	TFe_2O_3 (%)	CaO (%)	MgO (%)	K_2O (%)	Na_2O (%)	MnO (%)	TiO_2 (%)	P_2O_5 (%)	LOI (%)	Total (%)	CIA	ICV
Yalaguz Fm.	1	100913-01	shale	52.57	13.69	5.71	6.93	4.61	4.32	0.80	0.030	0.559	2.895	7.81	99.92	65	1.61
	2	100913-03	siltstone	67.31	15.29	4.00	1.73	0.23	4.00	2.66	0.072	0.494	0.124	3.98	99.89	60	0.92
	3	100913-04	siltstone	68.86	13.21	3.15	2.80	0.85	3.63	3.42	0.111	0.378	0.094	3.41	99.91	48	1.53
	4	100909-10	shale	61.55	14.03	5.96	2.77	3.44	3.41	1.95	0.091	0.677	0.150	5.83	99.87	58	1.66
	5	100913-06	shale	58.66	14.45	5.98	4.47	3.41	3.19	1.45	0.158	0.763	0.159	7.21	99.90	64	1.45
	6	100913-07	silty shale	23.99	6.13	1.45	31.83	2.14	0.55	2.64	2.022	0.217	0.068	28.21	99.25	40	3.68
	7	100909-06	shale	71.27	12.85	2.19	2.28	1.49	3.47	1.73	0.099	0.510	0.132	3.89	99.92	58	1.14
	8	100909-03	shale	64.25	16.03	5.63	0.36	2.03	4.37	3.01	0.026	0.698	0.195	3.30	99.88	62	0.82
Kelixi Fm.	9	100909-01	mudstone	63.52	19.02	3.13	0.61	2.23	5.01	1.01	0.025	1.016	0.215	4.14	99.92	71	0.61
	10	100910-13	shale	59.33	17.38	9.41	0.58	2.26	4.69	0.89	0.024	1.008	0.172	4.18	99.92	71	0.89
	11	100914-04	mudstone	58.08	15.06	10.50	1.91	2.60	3.88	1.05	0.058	1.187	0.193	5.38	99.90	66	1.22
	12	100914-02	mudstone	57.57	17.37	8.34	2.66	0.36	3.42	1.53	0.074	1.382	0.302	6.86	99.87	67	0.74
	13	100912-01	mudstone	55.55	20.10	9.34	0.26	1.75	6.84	0.61	0.022	1.392	0.063	3.90	99.84	69	0.73
	14	100910-11	shale	59.37	18.14	8.60	0.40	2.00	5.58	1.25	0.031	0.945	0.108	3.48	99.90	68	0.78
Yutang Fm.	15	100914-06	mudstone	67.95	15.57	3.46	0.48	1.98	4.85	2.14	0.034	0.641	0.164	2.61	99.89	63	0.85
	16	100914-07	mudstone	67.89	13.87	7.34	0.50	0.13	4.33	2.87	0.031	0.531	0.153	2.25	99.89	58	0.78
	17	100914-09	mudstone	66.13	18.08	2.31	0.36	2.31	5.64	0.57	0.016	0.592	0.074	3.85	99.92	71	0.73
	18	100914-10	mudstone	69.77	15.59	4.23	0.50	0.37	4.10	0.29	0.055	0.406	0.074	4.53	99.92	74	0.55
	19	100914-11	laminar shale	66.20	15.20	4.37	2.04	0.30	4.37	1.10	0.138	0.898	0.203	5.01	99.84	65	0.74
Kuerkake Fm.	20	100910-08	laminar siltstone	65.89	15.82	5.89	0.16	2.04	5.02	1.11	0.014	0.893	0.083	2.96	99.88	68	0.80
	21	100910-06	laminar siltstone	55.27	21.14	10.20	0.28	0.33	6.29	1.11	0.029	0.963	0.058	4.24	99.89	70	0.58
Kezisuh-umu Fm.	22	100910-03	mudstone	58.14	19.99	8.85	0.26	1.19	3.89	0.51	0.011	1.301	0.108	5.67	99.90	79	0.67
	23	100910-02	shale	54.83	22.18	8.98	0.21	1.13	4.23	0.35	0.033	1.430	0.120	6.39	99.90	81	0.62
	24	100914-14	mudstone	52.44	24.58	8.55	0.09	0.16	5.27	0.27	0.073	1.629	0.111	6.70	99.89	80	0.47
	25	100914-17	mudstone	55.01	16.13	9.11	2.46	3.63	3.09	1.40	0.109	1.262	0.224	7.48	99.90	67	1.37
	26	100914-22	shale	55.94	21.49	7.39	0.09	1.80	3.34	0.67	0.010	2.389	0.139	6.64	99.90	83	0.71

sents shallow lake facies belt. The greyish-green laminated siliceous siltstone, mudstone with mm-sized lamina and horizontal bedding with fine granularity and darker color represent deep lake facies belt.

3.3 Glacial facies

The Bolong Formation and Yutang Formation consist of amaranthine tillite, which is composed of moraine gravels and argilloarenaceous matrix. We interpret them as glacial facies. The massive diamictite shows no bedding and is poorly sorted. The size of gravels in the Bolong Formation varies in 5–10 cm and gradually turns smaller from the lower to upper part. Typical features of glacial sedimentation exist in the gravels, some of which present saddle shape, fissures and glacial striae because of pressure or friction (Figure 2(a), (b)). The size of gravels in the Yutang tillite is relatively small (mostly 1–2 cm) and the proportion of matrix increases in comparison to the Bolong tillite. Plate cross bedding, convolute lamination, and deformed bedding can be observed in the packsand or amaranthine gritstone, which overlie the tillite (Figure 2(f)), followed by greysih-green mudstone with sandstone lens, showing the characteristics of olistostrome (Figure 2(c)). Some big gravels bended or penetrated the laminas of laminated siltstone and formed the drop-pebble structure (Figure 2(e)), which supports a glacial-marine interpretation.

3.4 Littoral facies

Littoral facies is composed mainly of the Kelixi Formation of Nanhua System and Kuerkake Formation of Ediacaran System. The Kelixi Formation consists of two upward coarsening cycles (Figure 2(d)), and the littoral facies occurred on the top of each cycle. It mainly comprises purple quartzose gritstone and conglomerate. Plate crossbedding, wash crossbedding, and large-scale crescent type crossbedding can be found in the sandstone (Figure 2(g)). Diagonal beddings mainly consist of grit and packsand in radial arrangement. The conglomerate primarily shows massive bedding and the pebbles usually present imbricate pavement. The upper part of Kuerkake Formationm, which consists of purple and medium-thick layer sandstone and intercalations of silty shale, is characterized by littoral facies as well. Herringbone cross bedding can be observed in the pebbly sandstone (Figure 2(h)). It is interpreted as tidal-flat facies. Generally, those stratigraphic characteristics mentioned above reflect a littoral facies environment with a higher

Figure 2 Photos showing Neoproterozoic sedimentary features in Yecheng area. (a) Frozen crack of moraines gravel in the Bolong Fm.; (b) glacial striae; (c) olistostrome in the Yutang Fm.; (d) two coarsening upward cycles in the Kelixi Fm.; (e) dropstone structure; (f) convolute lamination in olistostrome; (g) diagonal bedding in the Kelixi Fm.; (h) herringbone cross bedding in the Kuerkake Fm.; (i) tepee structure in the sandstone of Kezisuhum Fm.

water power and a shallower water depth.

3.5 Neritic facies

The strata in the middle-lower part of each cycle of the Kelixi Formation and the middle-lower part of the Kuerkake Formation were formed in the neritic environment. The former consists of purple siltstone, silty shale, and fine grain clastic rocks. The surface of the green mudstone at the bottom appears moundy weathering and metaripple. Horizontal bedding has been found in the siltstone, which indicates a neritic environment in continental shelf with weaker hydrodynamic force. The latter consists of purple pebbly gritstone, quartz sandstone, and shale with horizontal bedding and low angle crossbedding. The granularity gradually turns fine upwards, representing a transitional environment from continental shelf margin to littoral facies.

3.6 Lagoonal facies

The Kezisuhum Formation is interpreted as lagoonal facies. It is composed mostly of purple packsand and yellow mudstone at the bottom and black siltstone interlayered with mudstone in the middle part. The thickness of each cycle is about 5 m. Tepee structure can be observed in the sandstone (Figure 2(i)). The granularity turns fine upwards on the whole. Horizontal bedding, sun crack in the black mudstone, and gypsum beds formed in the fissures of those rocks can be observed. In the upper part, it consists of thick-layer gritstone interlaminated with gypsum beds and black mudstone. These sedimentary features are the typical symbols of lagoonal facies.

4 Major elements analysis and discussion

Based on the major elements data, combined with the observation in field and the classification of sedimentary facies, we further analyzed the sedimentary tectonic setting and glacial periods, and compared them with coeval glacial events in other areas. One sample (100913-07) has been thrown out because of its high content proportion of CaO (31.83%) and LOI (28.21%).

4.1 Sedimentary tectonic setting

Roser and Korsch [38] divided three types sedimentary tectonic setting in the K_2O/Na_2O–SiO_2 discrimination diagram, i.e., passive continental margin (PCM), active continental margin (ACM), and arc [38]. All samples in the study area are projected in the field of passive continental margin (Figure 3). The previous researches show that dike swarm and bi-model volcanic rocks widely developed before the Nanhua Period and formed during the rifting of continent, and they are the early record of the break-up of Rodinia supercontinent [36], whereas our research indicates that the

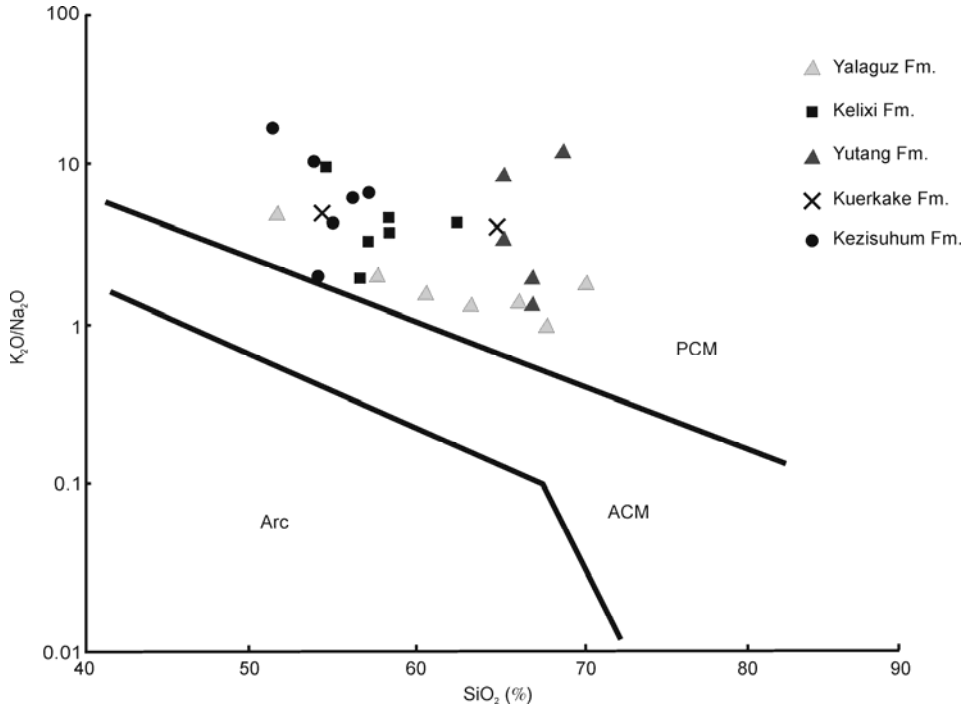

Figure 3 K_2O/Na_2O–SiO_2 discrimination diagram (modified from ref. [38]).

study area had turned into stable passive continental margin in the Nanhua-Ediacaran.

4.2 The applicability of the CIA

Chemical index of alteration (CIA) was put forward by Nesbitt and Young [39] in 1982 when they researched the clastic rocks in the Huronian Supergroup in Canada. It was used to reflect the degree of chemical weathering in source region, and infer the climate conditions when the source rocks formed. Afterwards, this index also was applied to discriminate the sedimentary environment, the components of source rocks, and diagenesis. Its expression is:

$$CIA=n(Al_2O_3)/[n(Al_2O_3)+n(CaO^*)+n(Na_2O)+n(K_2O)]\times 100.$$

All the oxidates are calculated in molecular proportions, where CaO^* is the amount of CaO incorporated in the silicate fraction of the rock [40]. Nessbitt et al. found that if the CIA values changed between 50 and 65, they indicate the systematic progression in alteration minerals tracks incipient. If the CIA values are between 65 and 85, they show intermediate chemical weathering. If the values are more than 85, they reflect extreme weathering intensity under warm and humid climate [39, 41, 42].

In addition, it is liable for sedimentary recycling and K-metasomatism to occur in the process of sediment transport and diagenesis. So, we should collect fine clastic rocks that can reflect the composition of source rocks as our samples, and besides the corrections for K-metasomatism and sedimentary recycling are also necessary. The K_2O addition to each weathered sample can be deducted according to $n_{pre}(K_2O)=n_{sample}(K_2O)-n_{add}(K_2O)$, where $n_{add}(K_2O)=[m\times n(Al_2O_3)+m\times(n(CaO^*)+n(Na_2O))]/(1-m)$, and $m=n(K_2O)/(n(Al_2O_3)+n(CaO^*)+n(Na_2O)+n(K_2O))$ [43]. We can use the index of compositional variability (ICV) to discriminate sedimentary recycling. It is usually used to judge whether the fine clastic rocks can represent the initial sedimentation.

$$ICV=[n(Fe_2O_3)+n_{pre}(K_2O)+n(Na_2O)+n(CaO^*)+n(MgO)+n(MnO)+n(TiO_2)]/n(Al_2O_3),$$

where CaO^* is the amount of CaO incorporated in the silicate fraction of the rock. When the ICV value is more than 1, it indicates that the sedimentary rocks contain relatively little clay minerals, belonging to the first-cycle sediments. When the ICV value is less than 1, the ICV value suggests that the sedimentary rocks have relatively abundant clay minerals and belong to recycling sediments or they once underwent intense chemical weathering [44, 45]. Most of the ICV values in our samples are more than 1 or close to 1 (Table 2), thus these samples are the initial sedimentary record.

Generally, those unstable elements like calcium, sodium and potassium are removed from the feldspars in upper crust by aggressive soil solutions so that the proportion of alumina to alkalis typically increases in the weathered product. The change of those elements in rocks, leading to deviate ideal weathering trend, can be shown on the $A(Al_2O_3)$-$CN(CaO^*+Na_2O)$-$K(K_2O)$ triangular diagram. Meanwhile, we can correct the CIA values resulting from

K-metasomatism through this diagram [46–48]. From Figure 4, we can find that most of samples show the phenomenon of K-metasomatism, especially those samples in the Kelixi Formation (Figure 4(b)). After corrected by the triangular diagram, these CIA values are in the range from 48 to 86, which are consist with those results from calculating (Table 2). In this diagram, those samples in the Yutang Formation show relatively disperse compared with the samples in other formations, and the CIA values range from 60 to 77, which suggests that the climate changed intensively at that time (Figure 4(c)). Besides, the projective point of the fresh rocks in provenance should start on the theoretical weathered path (the heavy arrow in Figure 4). So the point of intersection of theoretical weathered path and Pl-Kfs presents the proportion of feldspar. From Figure 4, the source rocks of our samples are granodiorite (Figure 4(a), (b), (d)) and granite (Figure 4(c)). They were probably derived from intrusive complex in the Heluositan Group in Archean. Two distinctive suites of magmatic intrusions were observed within the complex. The first was Akazi gneissic pluton of granodiorite and adamellite. The second suite, as represented by the Xuxugou pluton, has more complex composition than the first one. The principal rock types for the suite include granodiorite and granite (adamellite and K-feldspar granite) [49], which implies that those Nanhua-Ediacaran sediments in the study area may be derived from the same provenance. So we can get rid of the influence to the CIA values which results from the difference of source rock. Indirectly, it proves that the factor of climate influenced the CIA much more. The CIA, as one of the criteria to identify glacial period, is more acceptable [50].

4.3 Interpretation

Stratigraphic column and CIA values are shown in Figure 5. The CIA value (sample 100913-01) of purple shale interlayered with the polymicticconglomerate that occurred at the bottom of the Yalaguz Formation is 65 and 71 after correction, respectively, which implies a warm climate at that time. Those samples from the upper part of Yalaguz Formation have lower CIA values, ranging from 48 to 64 (samples 100913-04, 100913-03, 100909-10, 100913-06, 100909-06, 100909-03), with an average value of 59.3 (Figure 5(a)), which implies a colder climate. These lower CIA values in the Yalaguz Formation represent the beginning of the first glaciation in Neoproterozoic. Six CIA values from the Kelixi Formation range from 66 to 71 (samples 100909-01, 100910-13, 100914-04, 100914-02, 100912-01,

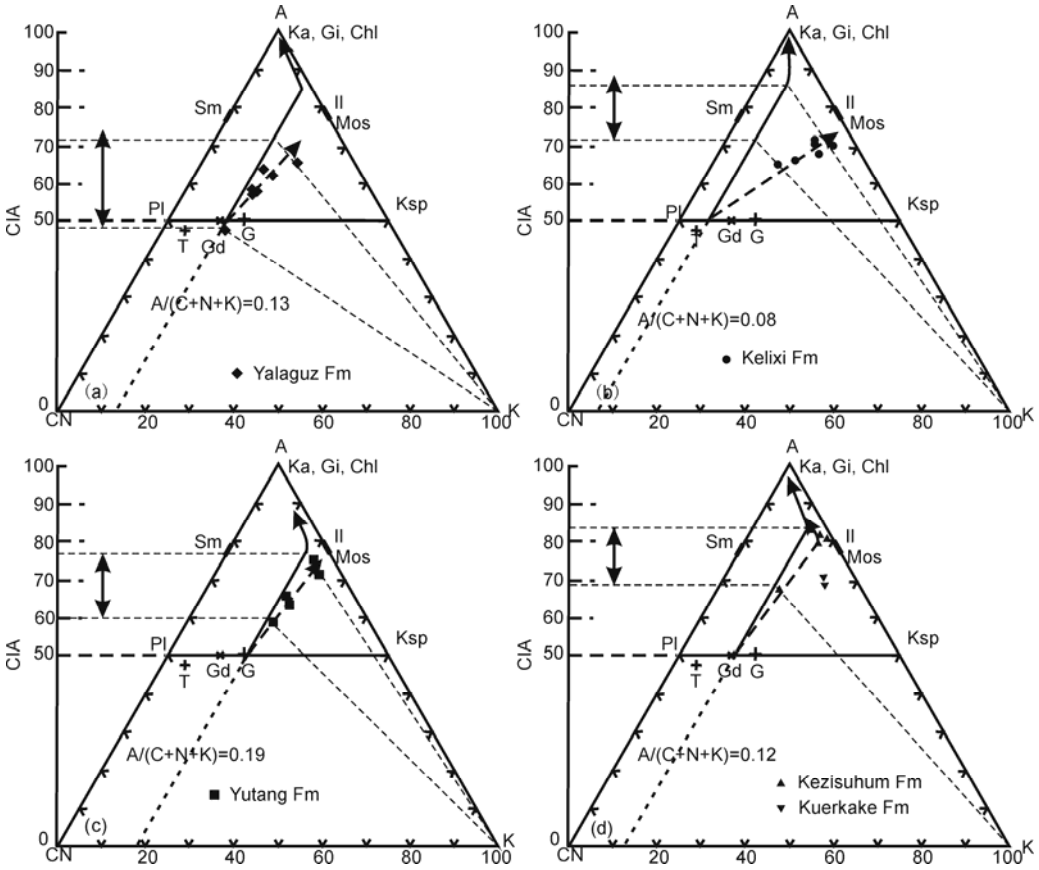

Figure 4 Ternary diagrams of A-CN-K. (a) Yalaguz Fm.; (b) Kelixi Fm.; (c) Yutang Fm.; (d) Kuerkake Fm. and Kezisuhum Fm. The heavy arrow indicates the theoretically weathered path, and the dotted arrow indicates the actually weathered path. A, $n(Al_2O_3)$; K, $n(K_2O)$; CN, $n(CaO^*+Na_2O)$; Ka, kaolinite; Gi, gibbsite Chl, chlorite; Sm, smectite; Ii, illite; Pl, plagiocalse; Kfs, K-feldspar; T, tonalite; Gd, granodiorite; G, granite.

100910-11), with an average value of 68.7 and their corrected values are in the range of 71–86, which indicates that the climate had changed to warmer and a medium-intense chemical weathering occurred under warm and humid climate conditions. Similar to the CIA values of the Neoproterozoic shale and pelite in the Bastar Craton [51], these strata formed littoral and neritic facies under warm climate. The CIA values of mudstone (samples 100914-06, 100914-07) above the Yutang Formation glacial diamictite are 63 and 58, respectively, and 64 and 60 after correcting (Figure 5(c)), implying a colder climate. But the CIA values of mudstone and shale (samples 100914-09, 100914-10, 100914-11) on the top of this formation are in the range of 65–74, suggesting climate changed to warmer again and a whole glacial period developed from glacial diamictite at the bottom to green mudstone on the top in the Yutang Formation. Two CIA values of purple siltstone (samples 100910-08, 100910-06) in the Kuerkake Formation are 68 and 70, respectively, representing tidal flat sedimentation under a warm and humid climate condition. The CIA values of samples (samples 100910-03, 100910-02, 100914-14, 100914-17, 100914-22) in the Kezisuhum Formation range from 67 to 83 (average 78), implying that the climate was warm even hot and the rocks underwent more intensive weathering.

To sum up, the CIA values in the upper part of the Yalaguz Formation are lower, with an average value of 59.3, representing the beginning of the first Neoproterozoic glaciation. The CIA values increase in the Kelixi Formation (average 68.7), implying that the climate became warm after the first glaciation. The CIA values of the Yutang Formation decrease to less than 65 (63 and 58 respectively), representing the second glaciation in Neoproterozoic. In contrast, all the CIA values in Eadicaran above the Yutang Formation are more than 65 and show gradually increased trend from the bottom to top, which means the study area was under a warm or hot climate condition in Ediacaran. Combined with the sedimentary facies analysis, two glacial events, called the Bolong glaciation and Yutang glaciation respectively, occurred during the Neoproterozoic in Yecheng area.

5 Correlation of strata and glaciations in different areas

Zhang et al. first set up the stratigraphic sucession in the study area after regional geological mapping in the late 1950s. Stratigraphic division was amended and Changcheng, Jixian and Qingbaikou systems were set up by Ma et al. in the 1980s. Meanwhile, the strata and their boundaries in Nanhua-Ediacaran were re-determined in terms of glacial deposition [34]. A few data were published from plutons and old metamorphic rocks under the Nanhua System [52–54], but it is difficult to correlate accurately the Neoproterozoic glacial-related strata between Quruktag and the study area. A rough correlation between study area and Quruktag by micropaleontologic fossils has been suggested. Abundant micropaleontologic fossils have been found in Quruktag, but just two micropaleotologic fossils, *Trachysphaeridium* sp. and *Taeniatum crasum* Sin, occurred in the Qiakemakelik Group including the Bolong Formation and Yutang Formation in the study area [55], and the two fossils had a long evolution history. Thus we cannot correlate glacial strata in the study area with coeval strata in other areas by micropaleontologic fossils correlations. But a large number of *Trematosphaeridium* sp., *Polyedryxium* sp., *Pseudozonosphaera rugosa*, etc., which firstly appeared in the Hankalchough Formation in Quruktag [56], have been found at the bottom of Kuerkake and Kezisuhum formations, which followed the Qiakemakelik Group [55]. Therefore, they are roughly equivalent to the Hankalchough or later formations. Furthermore, Li et al. [57] found that there was paleomagnetic mixed polarization in both the Qiakemakelik Formation (Group) and the Hankalchough Formation, and suggested that the two formations are correlated each other. So, the Kuerkake Formation that followed the Qiakemakelik Group should correspond to the horizons above the Hankalchough Formation.

Combined with the analysis of CIA values in the study area, we can make a further correlation (Figure 6). The CIA values in the upper part of the Yalaguz Formation are in the range of 48–62, which are almost consistent with those CIA values (48–61) of the Altungal Formation in Quruktag area [31], and as well correspond to those CIA values (58–61) of the upper Liantuo Formation below Nantuo glacial diamictite in South China [30]. Besides, the CIA values in the Kelixi Formation are 66–71 (average 68.7), which can be compared with the Yukengou and Shuiquan formations with CIA values of 67–76 (average 70.3) in Quruktag area. Therefore, we suggest that the Yutang glaciation can be correlated to the Hankalchough glaciation in Qurugtagh area, namely equivalent to the worldwide Gaskers glaciation [19], and because the top part of the Yalaguz Formation in the study area can correlate to the Altungal Formation, the Bolong glaciation is coeval with the Tereeken glaciation. Four glacial periods have been recognized in Quruktag area, including Bayixi glaciation of 740–732 Ma, Altungal and Tereeken glaciations of 725–615 Ma, and Hankalchough glaciation of 615–542 Ma [3, 19, 20, 58]. The Nantuo glaciation in South China was constrained between 663 and 635.4 Ma [11, 59], which can be correlated with the Tereeken glaciation [20] and then the Bolong glaciation according to the correlation of CIA values. Based on the chemical stratigraphic correlation of carbon isotope, He et al. [24] suggested the upper part of Qigbulak Formation in Aksu area can be correlated to the top part of the Dengying Formation in South China, the Sugetbulak Formation can correspond to the Doushantuo Formation, and the Yulmeinak Formation can be correlated to the Nantuo Formation. Thus the Bolong glaciation in Yecheng area also can be correlated to the Yulmeinak glaciation in Aksu area (Figure 6).

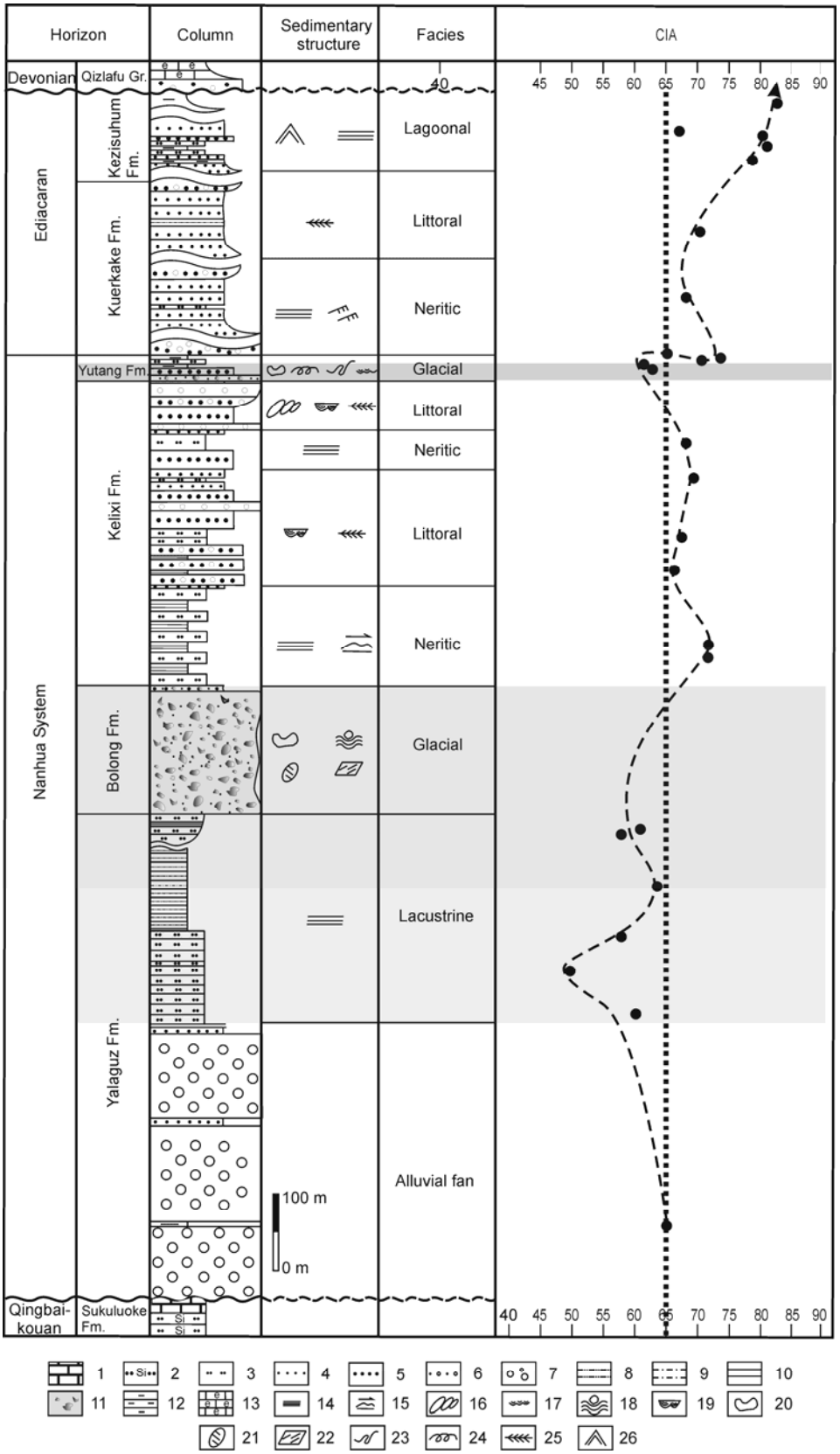

Figure 5 Neoproterozoic strata and CIA values in Yecheng area, Xinjiang. 1-Limestone; 2-siliceous siltstone; 3-siltstone; 4-medium sandstone; 5-gritstone; 6-pebbly gritstone; 7-conglomerate; 8-silty shale; 9-sandy shale; 10-shale; 11-tillite; 12-mudstone; 13-bioclastic limestone; 14-horizontal bedding; 15-metaripple; 16-imbricate structure; 17-deformed bedding; 18-dropstone structure; 19-crescent type cross bedding; 20-saddle structure; 21-frozen crack; 22- glacial striae; 23-slump bedding; 24- convolute bedding; 25- herringbone cross bedding; 26-tepee structure.

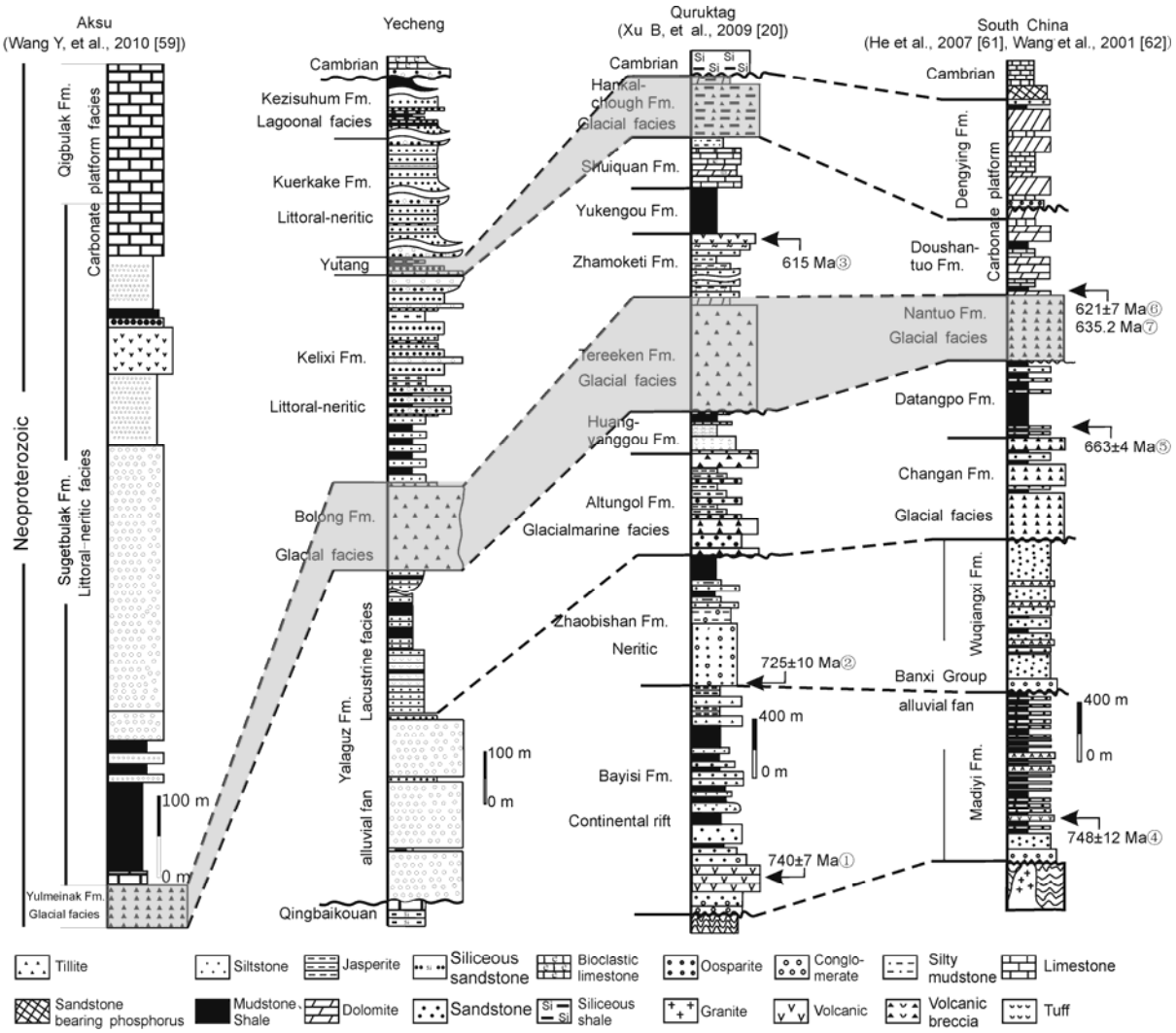

Figure 6 Correlation of stratigraphic sedimentary facies and glaciations in Neoproterozoic among Yecheng, Aksu, Quruktag and South China. ①–③ zircon SHRIMP U-Pb ages [20]; ④ zircon SHRIMP U-Pb ages [63]; ⑤ U-Pb TIMS ages [16]; ⑥ zircon SHRIMP U-Pb ages at the bottom of Liantuo Fm [12]; ⑦ U-Pb TIMS ages [11].

6 Conclusions

(1) Six sedimentary facies have been recognized in the study area, including alluvial fan, lacustrines, glacial, littoral, neritic and lagoonal facies, which shows that this area underwent a process from continent to marine, with mainly littoral and neritic sedimentation.

(2) Based on the analysis of CIA values, two cold events have been revealed in the study area, called the Bolong glacial period and Yutang glacial period, respectively.

(3) The Bolong glacial period in the study area can be correlated to the Yulmeinak glacial period in Aksu area, the Tereeken glacial period in Qurugtagh area and the Nantuo glacial period in South China. It is also equivalent to the Marinoan glacial period, which has been universally acknowledged. The Yutang glacial period can be correlated to the Hankalchough glacial period in Qurugtagh, which is equivalent to the Gaskers glacial period in Newfoundland.

Thanks for the assistance of Zhao Pan, Shi Guanzhong, Wang Yu and He Jinyou in the fieldwork. We gratefully acknowledge constructive reviews from two anonymous reviewers. This study was supported by National Natural Science Foundation of China (Grant Nos. 40972126 & 40821002).

1 Xu B. Recent study of the Rodinia supercontinent evolution and its main goal (in Chinese). Geol Sci Tech Inf, 2001, 20: 15–19
2 Zhang Q R, Chu X L, Zhang T G, et al. From global glaciation to snowball earth: Recent researches on the neoproterozoic glaciation events (in Chinese). Geol J China Uni, 2002, 8: 473–481
3 Li M J, Wang T G, Wang C G. "Snowball Earth" hypothesis and the palaeoenvironment for life evolution during the late Neoproterozoic (in Chinese). Acta Sed Sin, 2006, 24: 107–112
4 Zheng Y F. The Neoproterozoic magmatic activity and global change (in Chinese). Chin Sci Bull, 2003, 48: 1705–1720
5 Chu X L. "Snowball earth" during the Neoproterozoic (in Chinese). Bull Miner Petrol Geochem, 2004, 23: 233–238
6 Zheng Y F, Gong B, Zhao Z F, et al. Zircon U-Pb age and O isotope

evidence for Neoproterozoic low-^{18}O magmatism during supercontinental rifting in South China: Implications for the snowball earth event. Am J Sci, 2008, 308: 484–516
7 Hoffman P F, Kaufman A J, Halverson G P, et al. Comings and gongings of global galciation on a Neoproterozoic tropical platform in Namibia. GSA Today, 1998, 8: 1–9
8 Kaufman A L, Knoll A H, Narbonne G M. Isotopes, ice ages, and terminal Proterozoic earth history. Proc Natl Acad Sci, 1997, 95: 6600–6605
9 Fanning C M, Link P K. U-Pb SHRIMP ages of Neoproterozoic (Sturtian) glaciogenic Pocatello Formation, southeastern Idaho. Geology, 2004, 32: 881–884
10 Lund K, Aleinkoff J N, Evans K V, et al. SHIMP U-Pb geochronology of Neoproterozoic Windermere Supergroup, central Idaho: Implications for rifting of western Lauerntia and synchroneity of Sturtian glacial deposits. GSA Bull, 2003, 115: 349–372
11 Condon D, Zhu M, Bowring S, et al. U-Pb ages from the Neoproterozoic Doushantuo Formation, China. Science, 2005, 308: 95–98
12 Zhang S H, Jiang G Q, Zhang J M, et al. U–Pb sensitive high-resolution ion microprobe ages from the Doushantuo Formation in south China: Constraints on late Neoproterozoic glaciations. Geology, 2005, 33: 473–476
13 Key R M, Liyungu A K, Njamu F M, et al. The western arm of the Lufilian Arc in NW Zambia and its potential for copper mineralization. J Afr Earth Sci, 2001, 33: 503–528
14 Cailteux J L H, Kampunzu A B H, Batumike M J, et al. Lithostratigraphic position and petrographic characteristics of R.A.T. ("Roches Argilo-Talqueuses") Subgroup, Neoproterozoic Katangan Belt (Congo). J Afr Earth Sci, 2005, 42: 82–94
15 Bowring S, Myrow P, Landing E, et al. Geochronological constraints on terminal Neoproterozoic events and the rise of Metazoan. Geophys Res Abs, 2003, 5: 13219
16 Zhou C M, Tucker R, Xiao S, et al. New constraints on the ages of Neoproterozoic glaciations in south China. Geology, 2004, 32: 437–440
17 Chu X L, Zhang Q R, Chen F K, et al. Zircon U-Pb ages in the boundaries of Nanhua-Sinian (in Chinese). Chin Sci Bull, 2005, 50: 600–602
18 Kou X W, Wang Y, Wei W, et al. The Neoproterozoic Altungol and Huangyanggou formations in Tarim plate: Recognized newly glaciations and interglaciation (in Chinese)? Acta Petrol Sin, 2008, 24: 2863–2868
19 Xu Bei, Kou X W, Song B, et al. SHRIMP dating of the upper Proterozoic volcanic rocks in the Tarim plate and constraints on the Neoproterozoic glaciation (in Chinese). Acta Petrol Sin, 2008, 12: 2857–62
20 Xu B, Xiao S H, Zou H B, et al. SHRIMP zircon U–Pb age constraints on Neoproterozoic Quruqtagh diamictites in NW China. Precambrian Res, 2009, 168: 247–258
21 Gao Z J, Wang W Y, Peng C W, et al. The Sinian System of Xinjiang (in Chinese). Urumqi: Xinjiang Peoples's Publishing House, 1985. 1–123
22 Gao Z J, Chen K Q. The Nanhua System of Xinjiang and some geological issues of Nanhua System in China (in Chinese). Geol Surv Res, 2003, 26: 8–14
23 Chen P, Xu B, Zheng H F. The snowball earth hypothesis and the Neoproterozoic glacial events in Tarim block (in Chinese). Xinjiang Geol, 2004, 22: 87–93
24 He X B, Xu B, Yuan Z Y. C-isotope composition and correlation of the Upper Neoproterozoic in Keping area, Xinjiang (in Chinese). Chin Sci Bull, 2007, 52: 107–113
25 Dobrzinksi N, Bahlburg H, Strauss H, et al. Geochemical proxies applied to the Neoproterozoic glacial succession on the Yangtze Platform, South China. In: Jenkins, G L, McMenamin, M A S, McKay, C P, et al., eds. The Extreme Proterozoic: Geology, Geochemistry, and Climate. Geophy Monog Series, 2004, 146: 13–32
26 Rieu R, Allen P A, Plotze M, et al. Climatic cycles during a neoproterozoic "snowball" glacial epoch. Geology, 2007, 35: 299–302
27 Goldberg K, Humayun M. The applicability of the chemical index of alteration as a paleoclimatic indicator: An example from the Permian of the Paraná Basin, Brazil. Palaeogeo Palaeoclimat Palaeoecol. 2010, 293: 175–183
28 Feng L J, Chu X L, Zhang Q R, et al. CIA (chemical index of alteration) and its applications in the Neoproterozoic clastic rocks (in Chinese). Earth Sci Front, 2003, 4: 539–543
29 Feng L J, Chu X L, Zhang T G, et al. Liantuo sandstones: Sedimentary records under cold climate before the Nanhua big glaciations (in Chinese). Acta Petrol Sin, 2006, 22: 2387–2393
30 Wang Z Q, Yin C Y, Gao L Z, et al. The character of the chemical index of alteration and discussion of subdivision and correlation of the Nanhua system in Yichang area (in Chinese). Geol Rev, 2006, 5: 577–585
31 Liu B, Xu B, Meng X Y, et al. Study on the chemical index of alteration of Neoproterozoic strata in the Tarim plate and its implications (in Chinese). Acta Petrol Sin, 2007, 23: 2863–2868
32 Ding H F, Ma D S, Yao C Y, et al. Sedimentary environment of Ediacaran glacigenic diamictite in Guozigou of Xinjiang, China. Chin Sci Bull, 2009, 54: 3282–3294
33 Ma S P, Wang Y Z, Fang X L. The Sinian at north slope of western Kunlun Mountains (in Chinese). Xinjiang Geol, 1989, 7: 68–79
34 Ma S P, Wang Y Z, Fang X L. Basic characteristics of Proterozoic eonothem as a table cover on northern slope of the western Kunlun Mountains (in Chinese). Xinjiang Geol, 1991, 9: 59–70
35 Zhang C L, Ye H M, Zhao Y, et al. Geochemistry of the Neoproterozoic diabase and basalt in the south of Tarim plate: Evidence for the Neoproterzoic breakup of the Rodinia supercontinent in the south of Tarim (in Chinese). Acta Petrol Sin, 2004, 20: 473–482
36 Wang A G, Zhang CL, Zhao Y, et al. Depositional types of the lower part of Nanhua System on the northern margin of southwest and tectonic significance (in Chinese). J Strat, 2004, 28: 248–256
37 Zong W M, Gao L Z, Ding X Z, et al. Characteristics of Nanhua diamictite (tillite) and stratigraphic correlation in the southwestern margin of Tarim Basin (in Chinese). Geol China, 2010, 4: 1183–1190
38 Roser B P, Korsch R J. Determination of tectonic setting of sandstone-mudstone suites using SiO_2 content and K_2O/Na_2O ration. J Geol, 1986, 94: 635–650
39 Nesbitt H W, Young G M. Early Proterozoic climates and plate motions inferred from major element chemistry of lutites. Nature, 1982, 299: 715–717
40 McLennan S M. Weathering and global denudation. J Geol, 1993, 101: 295–303
41 Nesbitt H W, Young G M. Formation and diagenesis of weathering profiles. J Geol, 1989, 97: 129–147
42 Young G M, Nesbitt H W. Paleoclimatology and provenance of the glaciogenic Gowganda Formation (Paleoproterozoic), Ontario, Canada: A chemostratigraphic approach. Geol Soc Am Bull, 1999, 111: 264
43 Panahi A, Young G M, Rainbird R H. Behavior of major and trace elements (including REE) during Paleoproterozoic pedogenesis anddiagenetic alteration of an Archean granite near Ville Marie, Québec, Canada. Geochim Cosmochim, 2000, 64: 2199–2220
44 Cullers R L, Podkovyrov V M. Geochemistry for the Mesoperoterozoic Lakhanda shales in southeastern Yakutia, Russia: Implicationsfor mineralogical and provenance control and recycling. Precambrian Res, 2000, 104: 77–93
45 Cullers R L. The source and origin of terrigenous sedimentary rocks in the Mesoproterozoic Ui group, southeastern Russia. Precambrian Res, 2002, 117: 157–18
46 Wintsch R P, Kvale C M. Differential mobility of elements in burial diagenesis of siliciclastic rocks. J Sed Res, 1994, 64: 349–36
47 Fedo C M, Young G M, Nesbitt H W, et al. Potassic and sodic metasomatism in the Southern Province of the Canadian Shield: Evidence from the Paleoproterozoic Serpent Formation, Huronian Supergroup, Canada. Precambrian Res, 1997, 84: 17–36
48 Fedo C M, Young G M，Nesbitt H W. Paleoclimaticcontrol on the composition of the PaleoproterozoicSerpent Formation, Huronian Supergroup, Canada: A greenhouse to icehouse transition. Precambrian Res, 1997, 86: 201–223

49 Zhang C L, Li X H, Li Z X, et al. Neoproterozoic ultramafic–mafic-carbonatite complex and Granitoids in Quruqtagh of northeastern Tarim Block, western China: Geochronology, geochemistry and tectonic implications. Precambrian Res, 2007, 152: 149–169
50 Feng L J, Chu X L, Zhang Q R, et al. New evidence of deposition under cold climate for the Xiehuihe Formation of the Nanhua System in northwestern Hunan, China (in Chinese). Chin Sci Bull, 2004, 49: 1420–1427
51 Wani H, Mondal M E A. Petrological and geochemical evidence of the Paleoproterozoic and the Meso-Neoproterozoic sedimentary rocks of the Bastar craton, Indian Peninsula: Implications on paleoweathering and Proterozoic crustal evolution. J Asian Earth Sci, 2010, 38: 220–232
52 Zhang C L, Wang Z G, Shen G L, et al. Zircon SHRIMP dating and geochemistry characteristics of Akazi rock mass of western Kunlun (in Chinese). Acta Petrol Sin, 2003, 19: 523–529
53 Zhang C L, Yang C, Shen G L, et al. Zircon SHRIMP age of Neoproterozoic gneissoid granites in the western Kunlun and its significance (in Chinese). Geol Rev, 2003, 49: 239–244
54 Zhang C L, Lu S N, Yu H F, et al. Tectonic evolution of western Kunlun orogenic belt: Evidence from zircon SHRIMP and LA-ICP-MS U-Pb ages (in Chinese). Sci China Ser D-Earth Sci, 2007, 37: 145–154
55 Peng C W, Gao Z J. Microflora and stromatolites from the late Precambrian on the northern slope of west Kunlun mountains and their stratigraphic significance (in Chinese). Xinjiang Geol, 1984, 2: 17–28
56 Gao Z J, Zhu C S, Li Y A. Precambrian Geology in Xinjiang, China (in Chinese). Urumqi: Xinjiang Peoples's Publishing House, 1984
57 Li Y A, Gao Z J, W J H. Preliminary paleomagnetic study of Tarim late Precambrian paleo-block (in Chinese). Xinjiang Geol, 1984, 2: 81–93
58 Cao R G. New obversations of the Sinian system in the southern Yardang Mountains, Xinjiang (in Chinese). Geol Bull, 1991, 1: 30–34
59 Zhang S H, Jiang G Q, Han Y G. The age of the Nantuo Formation and Nantuo glaciation in South China. Terra Nova, 2008, 00: 1–6
60 Wang Y, He J Y, Wei W, et al. Study on the late Proterozoic sedimentary facies and sequence stratigraphy in Aksu area, Xinjiang (in Chinese). Acta Petrol Sin, 2010, 26: 2519–2528
61 He J Y, Xu B, Meng X Y, et al. Neoproterozoic sequence stratigraphy and correlation in Quruqtagh area, Xinjiang (in Chinese). Acta Petrol Sin, 2007, 23: 1645–1654
62 Wang J, Wang B J, Pan G T. Neoproterozoic rifting history of South China: Significance to Rodinia breakup. J Mineral Petrol, 2001, 21: 135–145
63 Ma G G, Li H Q, Zhang Z C. An investigation of the age limits of the Sinian System in South China. CAGS Bull Yichang Inst Geol Miner Res, 1984, 8: 1–29